9684 *Biochemistry* **2009,** *48,* 9684–9695
DOI: 10.1021/bi9013984

BIOCHEMISTRY
including biophysical chemistry & molecular biology
Article

N-Terminal Extension of βB1-Crystallin: Identification of a Critical Region That Modulates Protein Interaction with βA3-Crystallin

Monika B. Dolinska,[‡] Yuri V. Sergeev,*[,‡] May P. Chan,[‡] Ira Palmer,[§] and Paul T. Wingfield[§]

[‡]*National Eye Institute and* [§]*National Institute of Arthritis and Musculoskeletal and Skin Diseases, National Institutes of Health, Bethesda, Maryland 20892*

Received August 11, 2009; Revised Manuscript Received September 11, 2009

ABSTRACT: The human lens proteins β-crystallins are subdivided into acidic (βA1−βA4) and basic (βB1−βB3) subunit groups. These structural proteins exist at extremely high concentrations and associate into oligomers under physiological conditions. Crystallin acidic−basic pairs tend to form strong heteromolecular associations. The long N-terminal extensions of β-crystallins may influence both homo- and heteromolecular interactions. However, identification of the critical regions of the extensions mediating protein associations has not been previously addressed. This was studied by comparing the self-association and heteromolecular associations of wild-type recombinant βA3- and βB1-crystallins and their N-terminally truncated counterparts (βA3ΔN30 and βB1ΔN56) using several biophysical techniques, including analytical ultracentrifugation and fluorescence spectroscopy. Removal of the N-terminal extension of βA3 had no effect on dimerization or heteromolecular tetramer formation with βB1. In contrast, the level of self-association of βB1ΔN56 increased, resulting in homotetramer formation, and heteromolecular association with βA3 was blocked. Limited proteolysis of βB1 produced βB1ΔN47, which is similar to intact protein formed dimers but in contrast showed enhanced heteromolecular tetramer formation with βA3. The tryptic digestion was physiologically significant, corresponding to protease processing sites observed in vivo. Molecular modeling of the N-terminal βB1 extension indicates structural features that position a mobile loop in the vicinity of these processing sites. The loop is derived from residues 48−56 which appear to be critical for mediating protein interactions with βA3-crystallin.

Crystallins are the major structural proteins of the lens, where at very high concentrations they are responsible for the transparency and high refractive index (*1*). In the mammalian lenses, crystallins can be grouped into two families, small heat shock-related α-crystallins and βγ-crystallins (*1*, *2*). All βγ-crystallins are composed of two or more βγ-crystallin domains where each domain is made up of two β-stranded Greek key motifs. The β-crystallins are distinguished from γ-crystallins by having either N- and C-terminal extensions, for basic β-crystallins (βB1,[1] βB2, and βB3), or only an N-terminal extension, for acidic forms (βA1/A3, βA2, and βA4) (*3*, *4*). Whereas γ-crystallins exist as monomers, β-crystallins are known to associate into dimers, tetramers, and higher-order complexes under physiological conditions (*5*, *6*). On the basis of size-exclusion chromatography of lens extract, β-crystallins form three size classes of aggregates: βH (octamers of 160−200 kDa), βL_1 (tetramers of 70−100 kDa), and βL_2 (dimers of 46−50 kDa) (*7*, *8*). Intact βB1-crystallin is present only in the largest aggregate, βH, and absent in both dimeric βL_2 and the intermediate βL_1 (*9*−*11*). Lower-molecular mass aggregates contained only truncated forms of βB1 (*11*).

Because lens crystallins do not turn over with age, they are susceptible over time to a wide variety of post-translational modifications such as acetylation, deamidation, methylation, oxidation, phosphorylation, and truncation of terminal extensions by thiol proteases (*12*−*16*). These modifications may perturb protein stability and structure, enhancing further association and aggregation and leading to cataract development (*12*, *17*, *18*). Age-related proteolytic processing of human lens β-crystallins occurs mainly at the N-terminal extensions (*19*−*21*), and the first crystallins modified are βB1 and βA1/A3 (*17*, *19*−*21*). Processing of βB1 (also βA1/A3) was noticeable in < 1-year-old human lenses, and although the proportion of these truncated proteins increased with age, most had occurred by the age of 20 (*22*). Water-soluble high-molecular weight protein fractions of cataractous lenses also showed truncated βB1 and βA3 (*22*).

Earlier studies suggested that the N-terminal extension of β-crystallin played an important role in oligomerization (*23*). The role of these extensions in β-crystallin association has been studied by comparing the biophysical properties of N-terminally deleted variants with those of the intact protein. That these studies have not given a clearer picture is due among other things to the varying extent of the N-terminal deletions made. It was shown, for example, that residues 1−22 of the N-terminal extension of βA3 are not required for self-association (*24*);

*To whom correspondence should be addressed: OGVFB/NEI/NIH, 10B10, 10 Center Dr., Bethesda, MD 20892. Telephone: (301) 594-7053. Fax: (301) 402-1214. E-mail: sergeevy@nei.nih.gov.

[1]Abbreviations: βA3, human βA3-crystallin; βA3ΔN30, βA3 with residues 1−30 deleted; βB1, murine βB1-crystallin; βB1ΔN56 and βB1ΔN47, βB1 with residues 1−56 and 1−47 deleted, respectively; IPTG, isopropyl β-D-thiogalactopyranoside; SEC, size-exclusion chromatography; AUC, analytical ultracentrifugation; Tris, tris(hydroxymethyl)aminomethane; EDTA, ethylenediaminetetraacetic acid; DTT, 1,4-dithio-DL-threitol; TCEP, tris(2-carboxyethyl)phosphine hydrochloride; SDS−PAGE, sodium dodecyl sulfate−polyacrylamide gel electrophoresis; AEBSF (Pefabloc SC), 4-(2-aminoethyl)benzenesulfonyl fluoride hydrochloride; LC−MS, liquid chromatography−mass spectrometry; PTMs, post-translational modifications.

Published on Web 09/11/2009

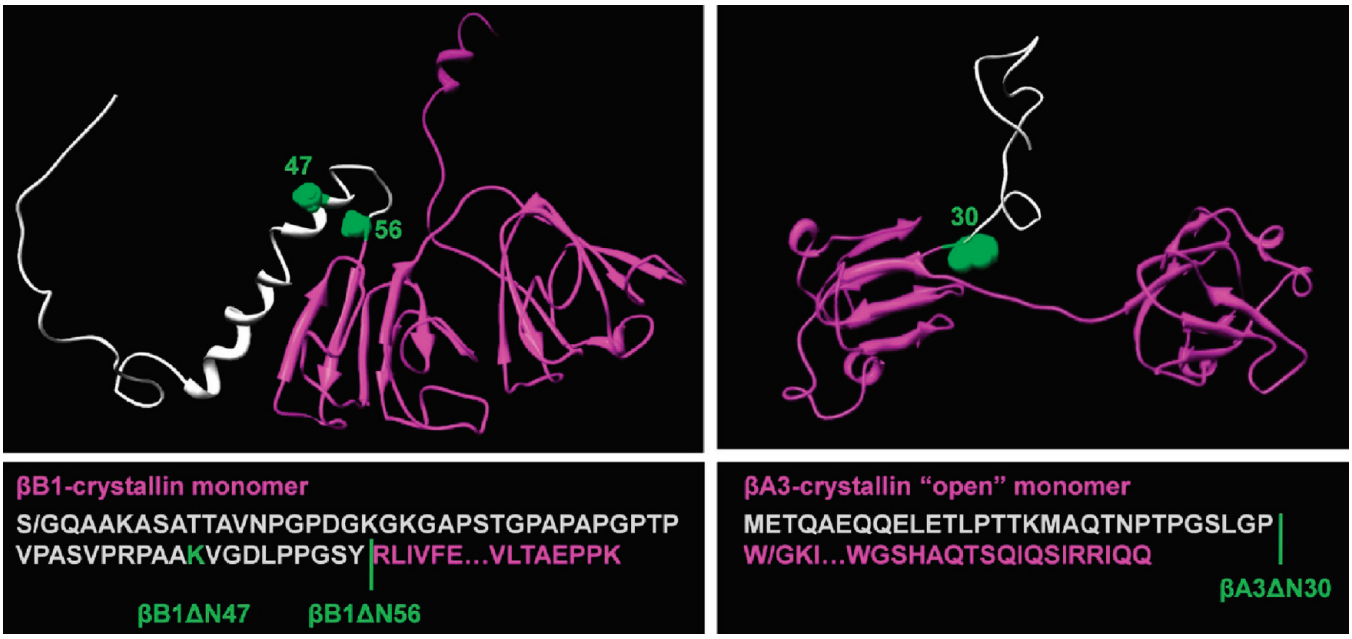

FIGURE 1: Three-dimensional models and sequences of βB1 and βA3 and N-terminal deletion variants. The models of murine βB1 and human βA3 were generated by homology modeling as previously described (*25*). In βB1, the N-terminal extension consists of four regions in which residues 1−28 are disordered, residues 29−41 and 43−47 form two short helical stretches, and residues 48−56 form a loop region connecting helix 2 and the main structural domain. The N-terminal extensions are colored gray, the sites of truncations green, and the core structures magenta. In βB1, S/G indicates mutation of Ser to Gly; in βA3, W/G indicates the mutation of Trp to Gly.

however, loss of residues 1−30 strengthens its tendency to self-associate (*25*) and significantly increases the enthalpy and entropy of binding relative to those of the full-length protein (*26*). Gupta et al. (*17*) showed that the loss of 21, 22, and 30 N-terminal residues resulted in oligomerization without changes in secondary structure. Also, truncated forms of βB1 with N-terminal deletions of 6 and 41 residues show increased levels of self-association as determined using light scattering (*27*). Removal of 41 N-terminal residues of βB1, which are extended outside the globular domain of the protein, has also been shown to suppress oligomerization and prevent protein crystallization (*28*). It has also been reported that deletion of 15 residues from the N-terminus of βB2 causes no apparent changes in its physical properties compared to those of the intact protein (*26*, *29*). However, deletion of 41 residues from the N-terminal arm of βB1 did not result in major structural alterations (*28*).

All acidic−basic pairs of β-crystallins, except βA4: βB's complexes, exhibit strong heteromolecular interactions (*30*), and in vivo, most β-crystallins are present as heterodimers (*31*). At low concentrations, βA3: βB2 form heterodimers (*6*, *32*) and at higher concentrations undergo further oligomerization to form heterotetramers (*6*, *9*). In the βA3: βB2 complex, both the flexible N- and C-terminal extensions of βB2 are solvent-shielded whereas the N-terminal extension of βA3 is solvent accessible (*6*). This suggests terminal extensions of βB2 play a role in formation of the heteromolecular complex. More recently, it was shown that deamidation of residues at the interface in the βA3 dimer decreased the extent of formation of the heterotetramer with βB1 and heterodimer with βB2 (*33*).

Previously, we demonstrated that βB1 and βA3 spontaneously form a reversible heteromolecular tetramer complex (*34*). In the work presented here, we used N-truncated forms of βA3 (βA3ΔN30) and βB1 (βB1ΔN56) to study the effects of the deletions on this association. To gain additional insight into the role of the N-terminal extension of βB1, we used limited proteolytic digestion to produce βB1ΔN47. Structural models and sequences of the crystallins described in the study are shown in Figure 1. Our results indicate that the N-terminal extensions stabilize the crystallins as their removal strengthens the tendency of both βA3 and βB1 to self-associate. Whereas βB1ΔN56 does not form heteromolecular complexes with βA3 (or βA3ΔN30), the tryptic digest βB12ΔN47 forms tight heteromolecular complexes with βA3. These results are discussed in relation to the structure of the N-terminal extensions and the in vivo processing of the crystallins.

MATERIALS AND METHODS

Expression and Purification of βB1 and βB1ΔN56. Murine βB1 was expressed and purified as described previously (*34*). The truncated mutant (βB1ΔN56), from which N-terminal residues 1−56 were deleted, was expressed using the pET/βB1ΔN56 plasmid in *Escherichia coli* strain BL21(DE3) pLysS (Invitrogen). While βB1 is expressed in *E. coli* cells as both soluble and aggregated (inclusion body) protein, βB1ΔN56 formed only inclusion bodies (Figure 2A, lanes P and S1). As we were unable to fold aggregated βB1ΔN56 extracted with urea or guanidine hydrochloride, we attempted to express βB1ΔN56 as a soluble protein. The effects of IPTG concentration (0, 0.1, 0.5, and 1.0 mM), temperature (16, 21, 28, and 37 °C), and induction time (0.5, 1, 2, 6, 12, 16, and 24 h) were studied, and optimum conditions for soluble protein expression were 0 mM IPTG, 21 °C, and 16 h (Figure 2A, line S2); however, the yield of soluble protein was still low compared to that of full-length βB1. Cells were harvested by centrifugation at 5000*g* and 4 °C for 15 min, and the pellets were resuspended in 50 mM Tris-HCl, 1 mM EDTA, 0.15 M NaCl, 1 mM DTT, and 50 μM TCEP (pH 7.5) (buffer A). The suspended cells were disrupted by sonication and centrifuged at 14000 rpm for 30 min at 4 °C. Briefly, purification of βB1ΔN56 was performed by DEAE

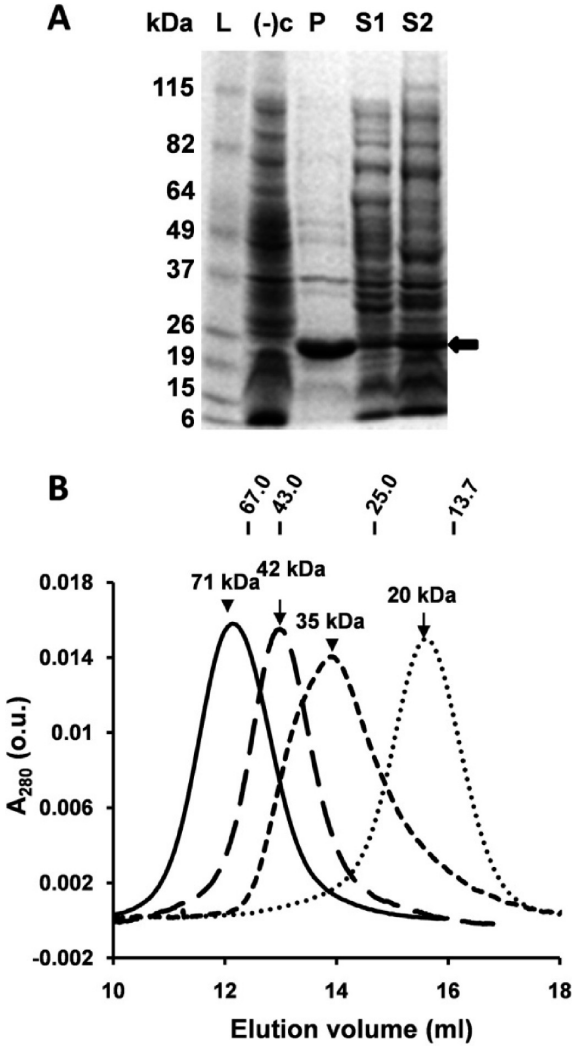

FIGURE 2: *E. coli* expression of β-crystallins and size fractionation of purified proteins. (A) SDS−PAGE of βB1ΔN56: lane L, molecular mass markers; lane (-)c, BL21(DE3) competent cells only; lane P, pellet (insoluble fraction); lane S1, supernatant (soluble fraction) with 1 mM IPTG at 37 °C for 2 h; lane S2, supernatant without IPTG at 21 °C for 16 h (βB1ΔN56 protein indicated by the black arrow). (B) Chromatography using Superdex 75 of βB1 (---), βB1ΔN56 (—), βA3 (− − −), and βA3ΔN30 (· · ·). Elution positions and molecular masses of protein standards are shown atop panel B.

anion-exchange, size-exclusion, and monoQ anion-exchange chromatographies. The purity and identity of βB1 and βB1ΔN56 were confirmed by SDS−PAGE and liquid chromatography chromatography−mass spectrometry, respectively.

Expression and Purification of βA3 and βA3ΔN30. Human βA3 and βA3ΔN30 were expressed as soluble proteins with high yields in *E. coli* and purified by anion-exchange and size-exclusion chromatography as described previously (*34*). In truncated βA3 (βA3ΔN30), N-terminal residues 1−30 were deleted and residue 31 was replaced with glycine (W/G). cDNA encoding βA3ΔN30 was cloned into pET-20b(+) and then used to transform competent BL21(DE3) cells (Invitrogen). Bacterial cultures were grown to an OD_{600} of 0.6−0.9 and induced for 2 h with 0.5 mM IPTG at 37 °C. The harvested cell pellet was resuspended in buffer A with complete protease inhibitor cocktail (Roche), sonicated on ice, and centrifuged. The supernatant was dialyzed overnight against 2 L of buffer B [50 mM Tris-HCl, 1 mM EDTA, 1 mM DTT, and 50 μM TCEP (pH 7.8)], then loaded on a 5 mL HiTrap DEAE FF anion-exchange chromatography column (GE Healthcare), and eluted with a gradient from 0 to 1 M NaCl in buffer B. Fractions (2.5 mL) containing βA3ΔN30 were pooled, concentrated, and applied to a 120 mL Superdex 75 HR16/60 SEC column previously equilibrated with buffer A at a flow rate of 0.5 mL/min, and 0.5 mL fractions were collected.

Tryptic Digestion of βB1. Murine βB1 (0.5 mg/mL) in 50 mM Tris-HCl, 150 mM NaCl, 1 mM EDTA, and 1 mM TCEP (pH 7.5) (buffer C) was incubated with 2.5% (w/w) trypsin (Trypsin Gold, Promega) for 8 min at 37 °C. The reaction was quenched with 2 mM AEBSF (Pefabloc SC, Roche), 1.5 M urea added, and the sample applied to a Superdex 200 column (1.6 cm × 50 cm) equilibrated with buffer C. The peak fractions were collected and analyzed by SDS−PAGE and mass spectrometry.

Liquid Chromatography−Mass Spectrometry (LC−MS). A HP1100 LC−MS electrospray mass spectrometer (Agilent) coupled to a Zorbac C-3, 2.1 mm × 15 cm column was used. Protein (~0.1−0.5 mg/mL) was diluted with H_2O or 10% formic acid to 1:20 to 1:50 and the sample (5 μL) applied to the column which was washed for 15 min with 0.1% formic acid and 5% acetonitrile, and then a 35 min gradient from 5 to 100% acetonitrile was applied. The flow rate was 0.2 mL/min, and the gradient eluate was analyzed by MS.

Circular Dichroism. Circular dichroism spectra were recorded in the far-UV region (185−260 nm) using a Jasco 500A spectropolarimeter and 0.02 cm path length cells. Samples were in 10 mM sodium phosphate buffer with 50 μM TCEP (pH 7.0). All spectra were averaged over 10 scans and were corrected by subtraction of a buffer blank. Mean residue ellipticities were expressed for all wavelengths as degrees square centimeters per decimole and were calculated from the equation $[\theta] = \theta_{obs} \times M/10 \times d \times c$, where θ_{obs} is the measured ellipticity in degrees, M the mean residue molecular mass (113, 116, and 117 kDa for βB1, βB1ΔN47, and βB1ΔN56, respectively), d the optical path in centimeters, and c the protein concentration in grams per milliliter.

Fluorescence Spectroscopy. Fluorescence emission spectra of individual and mixed crystallins (10 μM) were recorded after incubation for 0 and 24 h at room temperature in 10 mM sodium phosphate buffer and 50 μM TCEP (pH 7.0) with or without 8 M urea. Spectra were recorded using a Cary Eclipse fluorescence spectrophotometer (Varian). Proteins were excited at 285 nm, and the emission was recorded from 300 to 400 nm. The tryptophan analogue *N*-acetyl-L-tryptophanamide was used as a model for the intrinsic tryptophan emission.

Analytical Ultracentrifugation. Sedimentation equilibrium experiments were performed using a Beckman Optima XL-I analytical ultracentrifuge, absorption optics, an An-60 Ti rotor, and standard double-sector centerpiece cells. All analyses were performed using duplicate protein samples. Prior to a centrifugation, proteins, >95% pure as determined by SDS−PAGE, were incubated for 1 h at room temperature with 10 mM DTT and 1.5 M urea as previously described (*25*, *26*, *34*), dialyzed for 24 h at 4 °C against buffer A, and then adjusted to ~0.4 mg/mL. Data were collected after centrifugation for 16 h at 14500−17500 rpm and 20 °C. The baselines were established by overspeeding at 45000 rpm for an additional 3 h. Equilibrium profiles were analyzed by standard Optima XL-I Origin-based data analysis software. Solvent density was estimated as previously described (*35*). Monomeric molecular masses and molar extinction coefficients were used for calculation of dissociation constants

(K_d). M_r and K_d values were averaged from at least two experimental runs using duplicate samples.

Association Studies of β-Crystallins. Purified proteins were dialyzed overnight against buffer A in Slide-a-Lyser casettes (Pierce) at 4 °C. Protein concentrations were estimated from A_{280} using absorbancies calculated from cDNA sequences (NCBI entries NP_076184 for βB1 and NP_005199 for βA3) and adjusted to 0.5 mg/mL. Equimolar mixtures were incubated at room temperature. Aliquots for the SEC (250 μL) and native gel (10 μL) were sampled at various time points up to 24 h, immediately frozen in ethanol and dry ice, and stored at −80 °C.

(*i*) *Size-Exclusion Chromatography*. Aliquots (250 μL) of individual β-crystallins or crystallin mixtures were applied to an analytical grade 24 mL Superdex 75 HR10/30 column, precalibrated with low-molecular mass protein standards [bovine serum albumin (67 kDa), ovalbumin (43 kDa), chymotrypsinogen (25 kDa), and ribonuclease A (13.7 kDa) (Sigma)]. The column was equilibrated in buffer A and eluted at a flow rate of 0.5 mL/min, and 0.5 mL fractions were collected.

(*ii*) *Native gel electrophoresis* on 4 to 15% gradient Tris-glycine gels (Bio-Rad) was performed using 10 μL aliquots of protein controls or β-crystallin mixtures.

RESULTS

Expression and Physical Properties of β-Crystallins. In previous work, we showed that βB1 exhibited mixed expression in *E. coli* as both soluble protein and aggregated (inclusion body) protein were produced (*34*). Removal of the N-terminal extension resulted in expression of only the inclusion body protein (Figure 2A, lanes P and S1). Many proteins can be readily folded from denaturant-solubilized aggregates, but βB1ΔN56 was refractory to this approach. By modifying the expression conditions by, for example, using lower induction temperatures (*36*, *37*), we were able to generate soluble protein (Figure 2A, lane S2). Only the soluble fraction was used for protein purification and the biophysical studies described herein. The complete aggregation of expressed βB1ΔN56 was a first indication of the reduced solubility or instability compared to that of the wild-type protein. This has not been an issue before as only partially deleted N-terminal extensions were previously studied and these proteins were soluble when produced by in vitro proteolytic digestion (*5*, *38*) or recombinant expression (*27*, *28*, *39*) or directly isolated from the lens (*11*, *19*). Because of the protein's history, we carefully checked βB1ΔN56 for protein modification and conformational perturbation (described below). Mass spectrometry gave a mass of 22776.29 Da, consistent with the cDNA sequence that indicated the protein was intact and that no residues had been modified, factors that may lead to selective solubility during expression.

Gel filtration of βB1ΔN56 indicated an apparent molecular mass of ~ 75 kDa (Figure 2B) which is approximately twice that of homodimeric βB1 (35 kDa). Removal of the N-terminal extension clearly promotes higher-order protein association compared to that of the dimeric wild-type protein. A more detailed picture was obtained using sedimentation equilibrium analysis. Equilibrium profiles of βB1ΔN56 were best fitted to a monomer−tetramer system with a K_d of $(5.39 \pm 0.06) \times 10^{-17}$ M^3 and an average molecular mass of 74.6 kDa (Figure 3).

Removal of the N-terminal extension from βA3 had no effect on *E. coli* expression, and unlike βB1ΔN56, βA3 was expressed as a soluble protein. Sedimentation analyses of βA3ΔN30 indicated a monomer−dimer system similar to the wild-type protein although the truncation resulted in tighter dimer formation (Table 1).

Identification of a Flexible and Solvent Accessible Region of the βB1 N-Terminal Extension. As removal of the complete N-terminal extension of βB1 had such a profound effect on the physical properties of βB1, we asked if there was a minimal length or a cutoff point in this region that switches the behavior of the protein. As a simple first approach, the structure of βB1 was probed using limited proteolytic digestion. Trypsin was used because of its very reliable specificity and the fact that there is good distribution of basic residues throughout the protein. For example, in the N-terminal extension of the murine protein, there are basic residues at positions 5, 19, 21, 43, 47, and 57 (all these sites are matched in the human sequence except at position 43). The time course for digestion (Figure 4A) shows a single highly specific cleavage occurring in < 5 min. Mass spectrometry (LC−MS) determined that the digestion product had a mass of 23601.8 Da. This corresponded to residues 48−248 and showed that tryptic cleavage occurred C-terminal to lysine 47. This cleavage, which because of both the rate and selectivity must occur at an accessible and highly mobile region, is significant as it corresponds to the in vivo sites processed by gelatinase B (*40*) and m-calpain (*41*). Although the C-terminal region has been identified as being accessible to protease activity (*5*) under the condition used, we did not observe any major processing in this region with trypsin even after extended digestion times.

To study βB1ΔN47 in detail, we scaled up the tryptic digestion and isolated the processed protein by gel filtration (Figure 4B). Analysis by sedimentation equilibrium indicated a monomer−dimer system with a K_d of 1.4×10^{-6} M and an average molecular mass of 39.4 kDa (Figure 3), values similar to those of the wild-type protein (Table 1). This is in marked contrast to that of βB1ΔN56 which, as described above, undergoes further association to form tetramers (Figure 3).

Conformational Analyses of β-Crystallins. The far-UV circular dichroism spectra of βB1 and the two truncated variants, βB1ΔN56 and βB1ΔN47, all indicated predominately β-sheet secondary signatures characterized by low molar ellipticities and broad negative peaks (troughs) at ~214−215 nm (Figure 5). The small spectral difference between these proteins and the wild-type standard was eliminated by unfolding the proteins with 8 M urea (Figure 5). Thus, despite major differences in the physical properties of proteins with complete (Δ56) or partial (Δ47) deletions, no significant difference in the secondary structure was observed. There is also little structural perturbation between βA3 and βA3ΔN30 (*42*). Conformation was also probed using fluorescence emission, very sensitive to tertiary folding, using proteins (~10 μM) at concentrations higher than the K_d values of the associating systems (Table 1). Emission spectra of both βB1 and βA3 are red-shifted upon denaturation with concomitant ~2-fold increases in intensity (Figure 6). As exposure of buried tryptophan on unfolding normally decreases the emission intensity due to solvent exposure (higher polarity), in the native proteins there must have been quenching by neighboring residues. Unfolding the truncated variants (βB1ΔN47, βB1ΔN56, and βA3ΔN30) all resulted in red shifts in emission maxima, similar to those of their wild-type counterparts, with small, or no, increases in emission intensity (Figure 6). In both βB1 and βA3, there are no aromatic residues in the N-terminal extensions, so changes in Trp emission resulting from their removal must be either due to the removal of quenching residue(s) located in

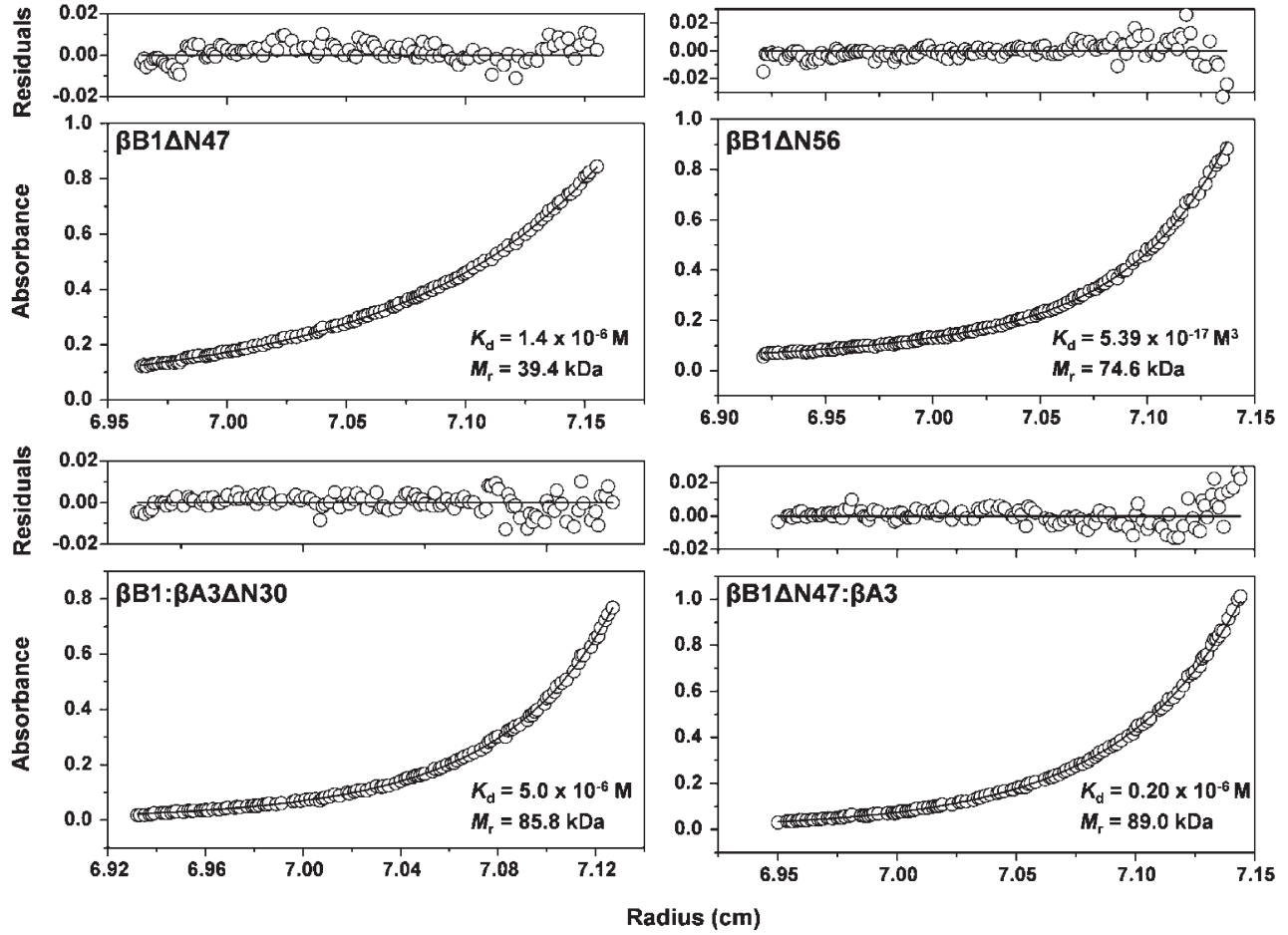

FIGURE 3: Sedimentation equilibrium of single and complexed β-crystallins. The protein concentration profiles, absorbance (280 nm) vs radial distance, are indicated. The solid lines indicate the predicted monomer−dimer (βB1ΔN47), monomer−tetramer (βB1ΔN56), and heterodimer−heterotetramer (βB1ΔN47: βA3 and βB1: βA3ΔN30) systems. White circles represent the experimental values. The top panels of each graph show the residuals of the fitted curves to the data points.

N-terminal extensions or due to local conformational shifts (Table 1).

The overall results of this section indicate that the global folding of the individual crystallin N-terminal variants is native-like with no major structural perturbations, but small localized conformational shifts cannot be ruled out, especially for βB1ΔN56.

Heteromolecular Association of β-Crystallins. (*i*) *βB1 Associates with βA3 or βA3ΔN30 to Form Heterotetramer Complexes*. Formation of a heteromolecular complex between βB1 and βA3ΔN30 was monitored by gel filtration and native gel electrophoresis. After incubation for 2 h, a single peak at ~70 kDa formed (Figure 7A) which corresponded to a single band of intermediate mobility on electrophoresis (Figure 7B). We previously demonstrated that βB1 and βA3 form a tetrameric complex by heterodimer−heterodimer association, and using this model, the association of βB1 and βA3ΔN30 was best fitted with a K_d of 5.0 μM (Figure 3 and Table 1). Therefore, although gel filtration showed the rate of complex formation was faster than that with wild-type βA3, the overall affinity appears weaker (*34*).

To examine potential conformational changes upon formation of the complex, fluorescence emission spectra of mixed proteins were compared with those of individual summed (nonmixed) samples. Both βB1: βA3 and βB1: βA3ΔN30 pairs exhibited blue-shifted spectra (5−8 nm) with reduced intensities (Figure 8). These changes are reminiscent of protein folding and indicate surface tryptophan shielding and quenching upon protein association and are analogous to those described for βB1 with βA1/βA3 and βA4 (*43*). From accessibility calculations for βB1 (*44*), four Trp residues are exposed or partially exposed, and in the homology model of βA3 (*26*), five Trp residues are exposed or partially exposed. Some of these surface tryptophan residues in the crystallin core structures must constitute part of the heterodimer interaction surfaces and provide a useful monitor of protein association.

(*ii*) *Formation of the βB1ΔN56 Tetramer is Suppressed in the Presence of βA3*. βB1ΔN56 did not interact with either βA3 or βA3ΔN30 as only the individual dimeric proteins were observed during gel filtration (Figure 7C). This is consistent with analytical ultracentrifugation that indicated noninteracting dimeric proteins (Table 1) and non-blue-shifted emission spectra (Figure 8). As there appears to be no stable interaction between these proteins, it was of interest that tetrameric βB1ΔN56, present when protein alone is analyzed, was not observed. One possibility is that heterodimers that are stable and do not undergo further association are formed. Native gel electrophoresis, however, shows that complex formation either is very slow or does not occur (Figure 7D). Alternatively, transitory heteromolecular interactions may occur, for example, at the surfaces (presumably hydrophobic) which mediate tetramerization of βB1ΔN56. Suppressed association may weaken over time as gel filtration peaks

Table 1: Physical Properties of Homo- and Hetero-Oligomers of Recombinant β-Crystallins

	calculated M_r[a]			AUC		
β-crystallin	monomer	dimer	SEC M_r[b]	M_r[c]	K_d (M)	association model (ref)
			Self-Association			
murine B1	28.0	56.0	35	47.3	1.5×10^{-6}	monomer−dimer (*34*)
murine B1ΔN56	22.9	45.8	71	74.6	5.4×10^{-17} M^3	monomer−tetramer
murine B1ΔN47	23.6	47.2	−	39.4	1.4×10^{-6}	monomer−dimer
human A3	25.1	50.2	42	42.6	4.5×10^{-6}	monomer−dimer
human A3ΔN30	21.9	43.8	20[d]	44.3	0.1×10^{-6}	dimer
murine A3	25.2	50.4	40	42.6	5.1×10^{-6}	monomer−dimer (*26*)
murine A3ΔN30	21.8	43.6	23[d]	42.7	0.7×10^{-6}	monomer−dimer (*26*)
murine B2	23.4	46.8	37	37.6	4.6×10^{-6}	monomer−dimer (*26*)
murine B2ΔN17	21.7	43.4	36	34.5	9.7×10^{-6}	monomer−dimer (*26*)
			Hetero-Association			
B1:A3	28.0:25.1	53.1	71	96.0	1.1×10^{-6}	dimer−tetramer (0.5−2 mg/mL) (*34*)
B1:A3ΔN30	28.0:21.8	49.8	70	85.8	5.0×10^{-6}	dimer−tetramer
B1ΔN56:A3	22.9:25.1	48.1	47	−	−	no association
B1ΔN47:A3	23.6:25.1	48.7	−	89.0	0.2×10^{-6}	dimer−tetramer
B1ΔN56:A3ΔN30	22.9:21.8	44.8	−	−	−	no association
B2:A3	23.4:25.2	48.6	49	50.0	−	heterodimer (< 1 mg/mL) (*6*)
B2:A3	23.4:25.2	48.6	−	90.0	−	heterotetramer (> 1 mg/mL) (*6*)

[a]Polypeptide molecular masses in kilodaltons were calculated from the protein sequences (consistent with NCBI entries NP_076184 for βB1, NP_005199 for βA3, and and NP_031799 for βB2). Murine βA3 and βB2 are 95 and 97% identical with their human species, respectively, with ~50% sequence identity shared among the pairs of β-crystallins independently on species; the globular domains of human and murine βB1-crystallin are ~80% identical and ~92% similar in terms of their amino acid properties, which provide a reasonable basis for comparison of a role of their globular domains and terminal extensions in β-crystallin association (*34*). [b]Apparent molecular masses in kilodaltons analyzed by size-exclusion chromatography. [c]Weight-average molecular masses in kilodaltons determined by AUC; K_d dissociation constants from analytical ultracentrifugation. The wild-type and truncated βB1 and βA3 were expressed in *E. coli* (*34*), and βB2 was expressed in a baculovirus system (*26*) or isolated from bovine lenses (*6*). [d]Proteins which elute via SEC as apparent monomers because of the interaction with the column matrix.

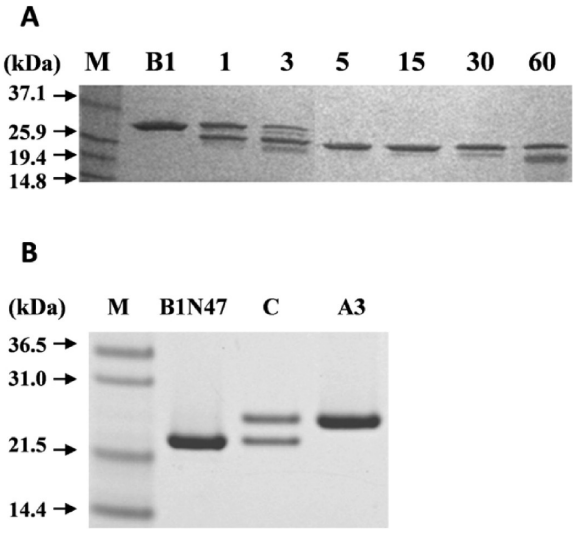

FIGURE 4: Tryptic digestion of βB1. Analytical scale time course and preparative scale. (A) SDS−PAGE of tryptic digestion of βB1 (B1) with 2.5% (w/w) trypsin (times in minutes). Black arrows indicate the molecular mass of the protein marker (M). (B) SDS−PAGE of large-scale βB1 tryptic digestion followed by gel filtration purification: βB1ΔN47 (B1N47), equimolar mixture of βB1ΔN47 and βA3 incubated for 24 h at room temperature (C) and used for analytical ultracentrifugation, and βA3 used for complex formation studies (A3).

of the unresolved homodimers shift to higher masses with extended preincubation times, where the leading edge of the peak is more populated with βB1ΔN56 than βA3 despite its lower monomer mass (Figure 7C).

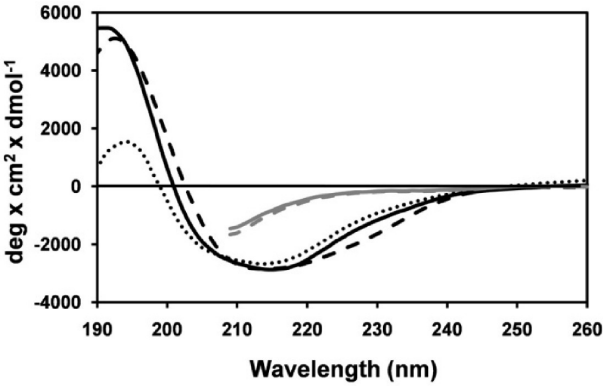

FIGURE 5: Far-UV circular dichroism spectra of βB1-crystallins. Samples were in 10 mM sodium phosphate (pH 7.0). Data for βB1, βB1ΔN56, and βB1ΔN47 are indicated by black solid, dashed, and dotted lines, respectively. Data for βB1 and βB1ΔN56 unfolded with 8 M urea are indicted by gray solid and dashed lines, respectively. Full far-UV spectra of unfolded proteins are not shown because the absorption by 8 M urea precludes measurements below 210 nm (*56*).

(*iii*) *βB1ΔN47 Associates with βA3 to Form a Stable Heterotetramer Complex*. We have seen that truncation of the N-terminal extension of βB1 abrogates its ability to undergo heteromolecular interaction with βA3-crystallin while at the same time strengthening its tendency toward higher-order self-association. The removal of more than 80% the βB1 extension by limited tryptic digestion, however, does not impair heteromolecular association but results in tighter complex formation. The association of βB1ΔN47 with βA3 was assessed by sedimentation equilibrium and corresponded to a heterodimer−heterodimer (tetramer) association (Figure 3). The K_d (0.2×10^{-6} M) of the

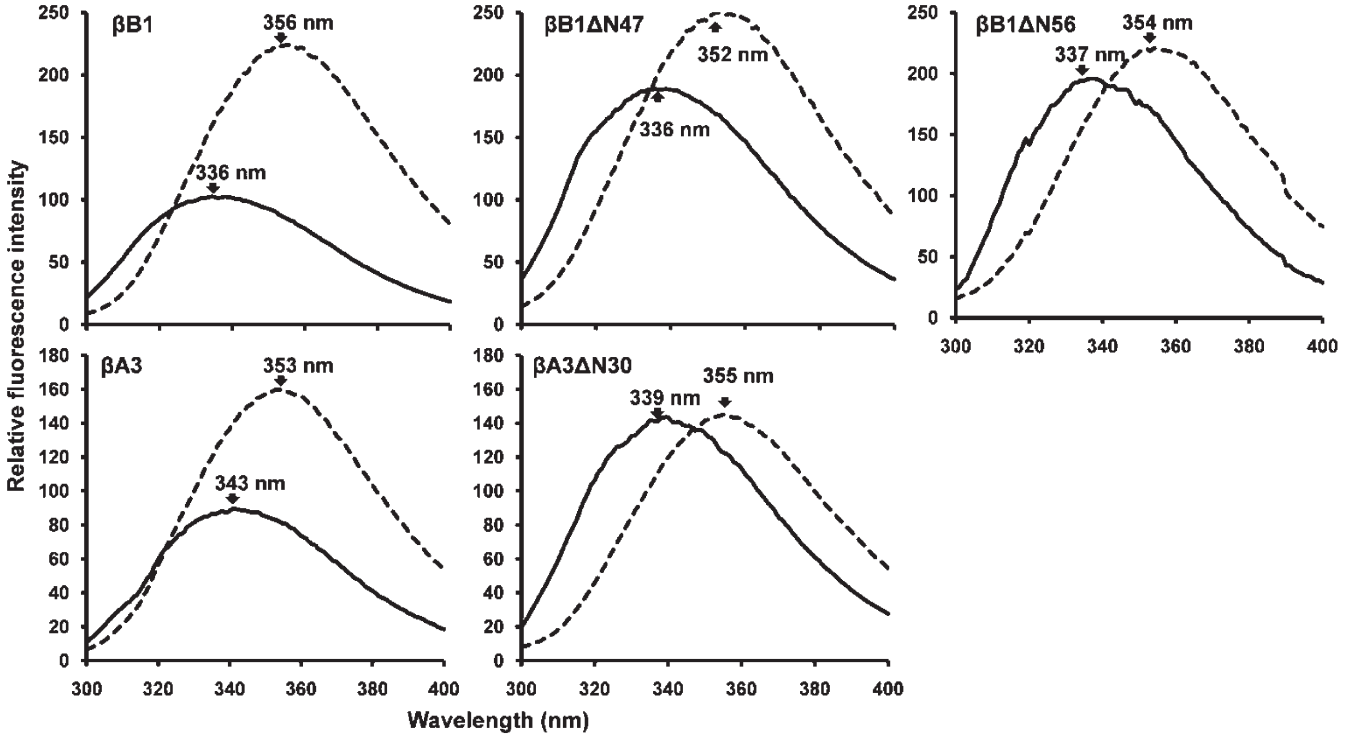

FIGURE 6: Tryptophan fluorescence emission spectra of βB1 and βA3 and N-terminal deletion variants. Data for native and unfolded proteins are indicated by solid and dotted lines, respectively. Proteins were excited at 285 nm and emission spectra recorded from 300 to 400 nm. Proteins (10 μM) were in 10 mM phosphate buffer (pH 7.0) and 50 μM TCEP with or without 8 M urea.

system indicated an affinity 5-fold stronger than that previously reported for unmodified βB1 (*34*). Heteromolecular complex formation was also demonstrated by fluorescence spectroscopy which shows a characteristic blue-shifted emission spectrum, almost identical to that of the βB1: βA3 complex (Figure 8).

(*iv*) *Summary of Molecular Interactions*. A schematic overview of the main findings of this study is summarized in Figure 9, and the physical properties of various individual and complexed recombinant crystallins, both from this study and from those previously published, are given in Table 1.

DISCUSSION

The available crystallin structures βB1 and βB2 [Protein Data Bank (PDB) entries 1blb and 1oki] do not include the N-terminal extensions but on the basis of their susceptibility to both in vivo and in vitro protease processing are likely to be solvent accessible, flexible, and probably unstructured (*38*, *44*, *45*). Although we cannot directly assign structure to these regions, on the basis of homology modeling they may include microdomains with helical structure (*16*) (Figure 10). Related to the lack of structural detail is the fact that functional roles of N-terminal extensions are also unclear despite much study. That they stabilize crystallin structure is suggested by their partial removal often leading to strengthened protein association and aggregation (*25*, *27*, *38*, *46*). This is complicated by the fact that crystallins exist as complexes and N-terminal modifications may also stabilize or destabilize heteromolecular interactions (*6*, *9*, *31*). To clarify the role of the N-terminal extensions of the two major eye lens crystallins βB1 and βA3, we prepared recombinant deletion mutants corresponding to the boundaries of the core structures of these proteins. The physical and conformational properties of these mutants, βA3ΔN30 and βB1ΔN56, lacking 30 and 56 N-terminal residues, respectively, were studied. Specifically, we used analytical ultracentrifugation for the direct determination of molecular masses and equilibrium binding constants (summarized in Table 1). Fluorescence emission measurements were useful both for assessing the conformational integrity of the individual N-terminal deletion mutants (Figure 6) and for monitoring their heteromolecular protein interactions (Figure 8).

Crystallin N-Terminal Extensions Mediate Protein Interaction. From the results of this study, it is clear that removal of the N-terminal extension of βB1 has major effects on the physical properties of the protein by increasing the self-association potential and by blocking heteromolecular associations with βA3 (*34*) (Figures 3 and 7). On the other hand, removal of the N-terminal extension of βA3 has little effect on either its dimerization potential or its ability to complex with βB1. Formation of a complex between βA3 and βB2 also indicates a lack of involvement of the N-terminal extension of the former which remains solvent accessible (*6*). The long 56-residue N-terminal extension of βB1 may directly interact with βA3 at the dimer interface, allowing the formation of heterodimers that then further associate into tetramers. This type of "holdase" role of terminal extensions has been discussed earlier for other proteins (*47*), and although we do not have direct structural evidence of such a role in βB1, we have shown that its removal abrogates heteromolecular interaction with βA3.

Apart from potential direct interactions, the presence or absence of the N-terminal extensions may have other consequences, namely, shifting the balance between so-called "closed" and "open" conformational isomers (*25*). The open conformation was determined experimentally for βB2 (PDB entry 1blb) (*48*). Later it was experimentally confirmed that β-crystallins might adopt the closed conformation as shown in the structure of βB1 (PDB entry 1oki) (*44*). Hence, in βB1, the large N-terminal arm could affect the kinetics and equilibrium position of these two conformations. This would be important if

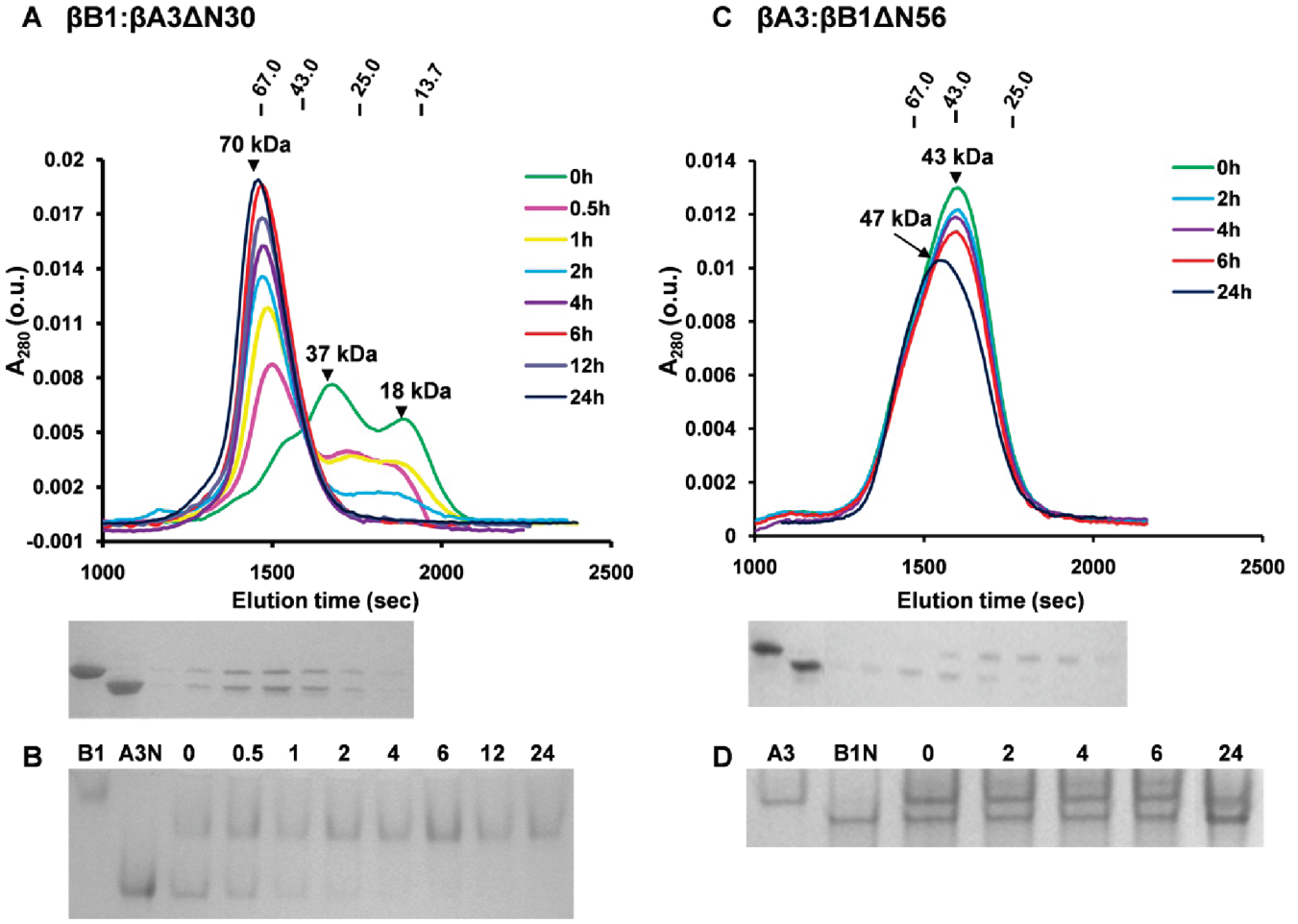

FIGURE 7: Size-exclusion chromatography and native gel electrophoresis of crystalline complexes. (A) Chromatography of a 18 μM equimolar mixture of βB1 and βA3ΔN30 preincubated for the indicated times (hours). Molecular masses of major peaks were estimated to be 18 and 37 kDa at 0 h and 70 kDa at > 2 h. Molecular masses of standards are atop the panel. SDS−PAGE of the fractions from the 24 h chromatogram is shown below the chromatograms, where lanes 1 and 2 contained βB1 and βA3ΔN30 standards, respectively. (B) Native gel electrophoresis of a βB1 and βA3ΔN30 mixture incubated for the indicated times (hours), where lanes 1 and 2 contained βB1 and βA3ΔN30, respectively. (C) Chromatography of a 18 μM equimolar mixture of βA3 and βB1ΔN56 with matching SDS−PAGE gel of the fractions from the 24 h chromatogram, where lanes 1 and 2 contained βA3 and βB1ΔN56, respectively. (D) Native gel electrophoresis of the βA3 and βB1ΔN56 mixture incubated for the indicated times (hours), where βA3 and βB1ΔN56 standards are indicated.

one conformation presented a favored interface for interaction with βA3.

Although N-terminal arms of crystallins may directly affect the first step in association pathways, namely, homodimer and/or heterodimer formations, other interfaces in the main core domains are probably more important for mediating higher-order associations. This is indicated by the blue-shifted fluorescence emission accompanying formation of a complex between, for example, βB1 and βA3 and is due to solvent shielding of surface Trp residue(s) on core domains (Figure 8). While removal of the N-terminal extension from βB1 results in higher-order self-association to form a homotetramer (Figure 8), heteromolecular interactions with βA3 are blocked. If we assume a homotetramer is formed by dimer−dimer association, the interface between dimers is likely to be similar to that which stabilizes hetero-tetramers. Future determination of the structure of heteromolecular complexed crystallins will provide the detailed information presently lacking.

Structural Basis of N-Terminal Extension Processing. It is well-documented that the N-terminal extensions of crystallins are very susceptible to in vivo proteolytic processing (*40*, *49*−*51*); however, it is less clear which proteases are physiologically significant and what, if any, are the triggering mechanisms. On the basis of the dramatic effects of completely removing the N-terminal of βB1, we were concerned that although the deleted sequence conformed to the structural domain determined by protein crystallography (*44*) it had no physiological relevance as no in vivo processing at this site has been reported. Other groups, however, have also considered fully N-terminally truncated βB1 relevant, and indeed while we were preparing this paper, a report appeared showing that truncated βB1 had degraded physical properties, including an inability to form a complex with βA3 (*52*). As different techniques and His-tagged proteins were used in this study, it is difficult to compare in detail these results with our data.

As complete removal of the N-terminal domain of βB1 has such a large impact on its physical properties, we were interested in defining more precisely the structural boundaries of the N-terminal region. This cannot be approached directly because as mentioned, the N-terminal domains are not included in any X-ray models, so limited proteolytic digestion is an obvious first choice given the sensitivity of this region to in vivo processing (*40*, *44*, *45*, *51*). We have described the remarkable selectivity with which tryptic processing of βB1 occurs, resulting in deletion of

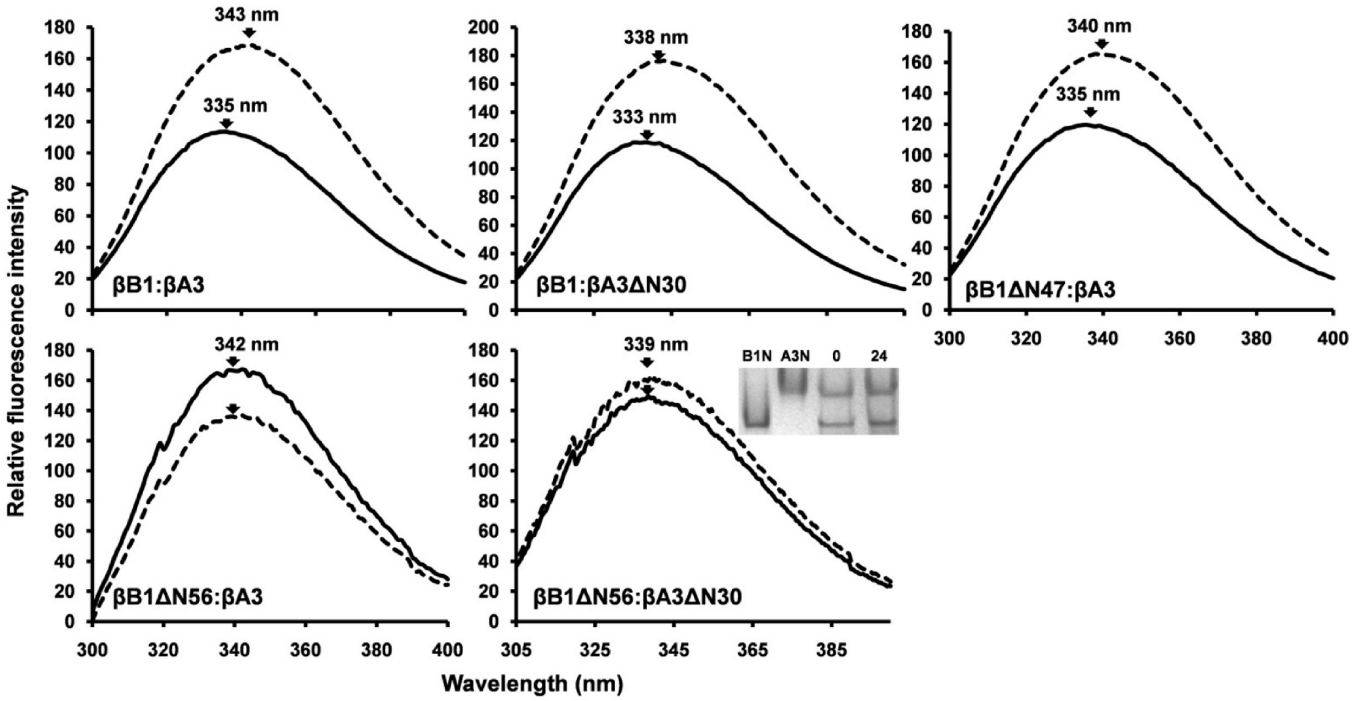

FIGURE 8: Tryptophan fluorescence emission spectra of β-crystallin complexes. Spectra of equimolar mixtures following a 24 h incubation are indicated by solid lines and the corresponding summed spectra of the individual (nonmixed) β-crystallin pairs by dotted lines. The inset shows native gel electrophoresis of βB1ΔN56 and βA3ΔN30 incubated for 0 and 24 h; B1N and A3N refer to βB1ΔN56 and βA3ΔN30, respectively.

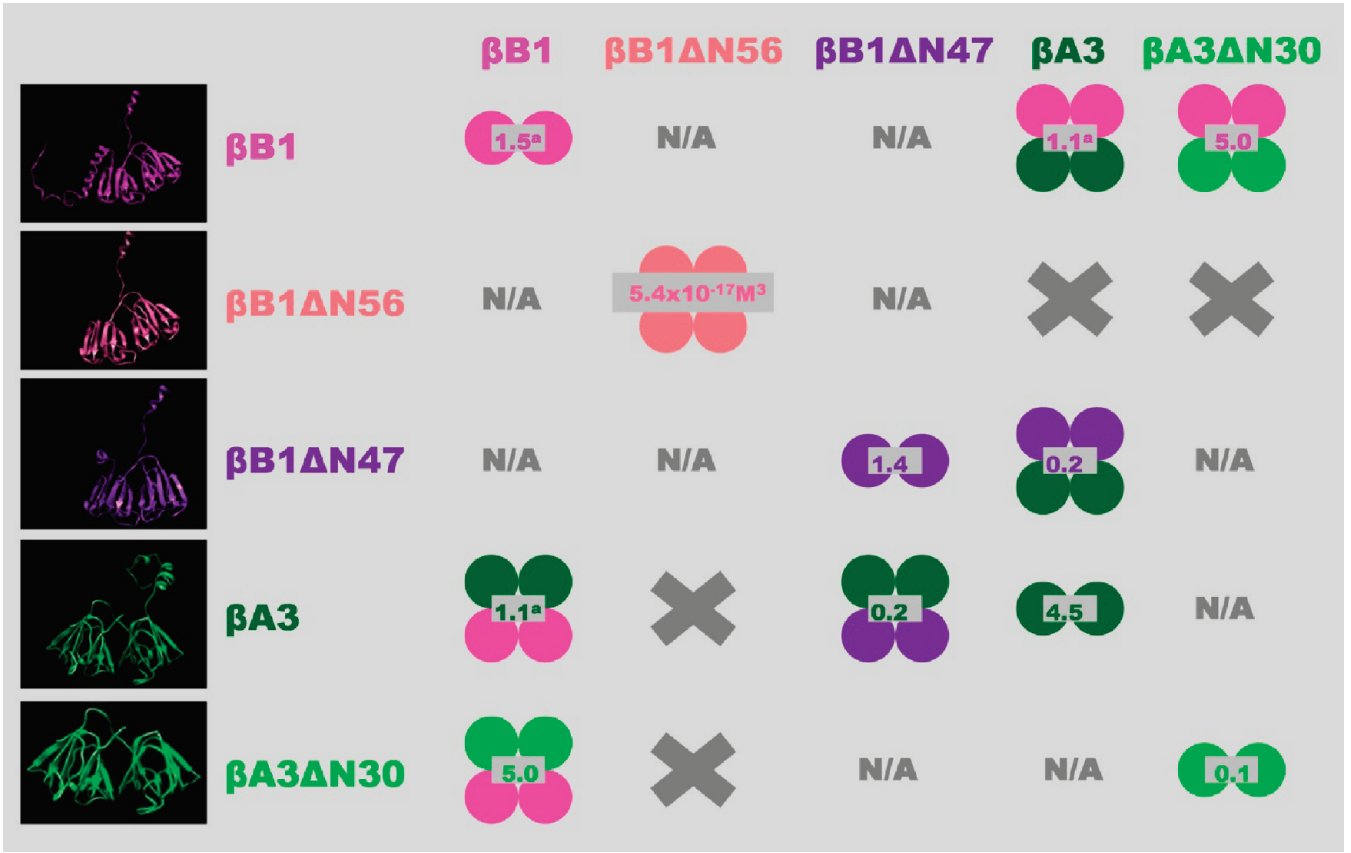

FIGURE 9: Overview of β-crystallin homo- and heteroassociation. The indicated shifts in the oligomeric equilibria as a result of N-terminal truncations may also occur in the lens, but this is difficult to prove directly due to the high in vivo protein concentrations. Some support for this, however, is the fact that the proteolytic processing of crystallins causes cataract formation in mice (*40*). Single circles represent monomeric units. Homo-oligomers are shown in single colors, and hetero-oligomers are bicolored. Values in gray indicate dissociation constants (K_d) in micromoles (except for βB1ΔN56). The left panel show β-crystallin models from top to bottom: full-length βB1 and βB1 with N-terminal truncation of 56 (βB1ΔN56) and 47 (βB1ΔN47) residues and full-length βA3 and βA3 with N-terminal truncation of 30 residues (βA3ΔN30). An X indicates no association between indicated β-crystallins. N/A indicates the interaction was not characterized. Values followed by a superscript a were previously determined (*34*).

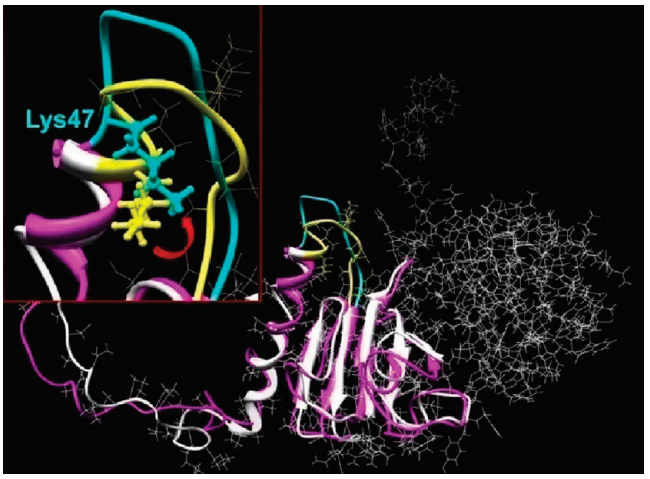

FIGURE 10: Molecular model of the βB1 N-terminal extension. The murine βB1-crystallin structure was determined using homology modeling and human truncated βB1-crystallin (PDB entry 1oki) as the structural template. Hydrogen atoms were added to the structure which was regularized using OPLS_2005 potentials with 12 Å nonbonded cutoffs. Molecular dynamics in water were performed with the Impact module of Maestro version 8.0.308 (Schrödinger Inc., New York, NY). The initial structure of the βB1 monomer is depicted as white ribbons and after MD equilibration for 20 ps as pink ribbons (details shown for residues 1−142). The inset shows structural details of residues 47−56 where the initial and equilibrated structures are colored yellow and cyan, respectively. The location of the tryptic cleavage site (between K47 and V48) is indicated by the ball-and-stick rendition, and the red arrow shows the approximate direction of Lys47 and the peptide movement.

more than 80% of the N-terminal extension (Figures 1 and 4). The trypsin-digested product βB1ΔN47 retained the physical properties of the intact protein exhibiting stable monomer−dimer association and also the ability to form stable heteromolecular tetramer complexes with βA3 (Figure 3). We note that the deletion proteins, βB1ΔN47 and βB1ΔN56, do not have a stable oligomeric structure at low protein concentrations as they are in dynamic equilibria where monomers and dimers are associating and dissociating. Therefore, there is no difference in the effect of the N-terminal extension on association for mutant proteins prepared by either site-directed mutagenesis or proteolytic digestion. It is also of interest, that the circular dichroism spectrum of βB1ΔN47 is very similar to that of βB1ΔN56 (Figure 5), and deconvolution of either spectrum indicates an apparent change in secondary structure compared to that of the wild-type protein (data not shown). However, this difference cannot account for the altered physical properties, as βB1ΔN47 behaves like the wild-type protein. More likely, they point to the difficulties in estimating the secondary structure of proteins with high β-sheet content (*53*) and the fact that the N-terminal domain is partially structured.

The selectivity of the tryptic digestion may be explained on a structural basis (Figure 1). Molecular modeling suggests that the βB1 N-terminal extension comprises an unstructured region (residues 1−28), two helical segments (residues 29−41 and 43−47), and a looplike domain (residues 48−56). In contrast to typical α-helices, which are saturated with hydrogen bonds, the stability of the N-terminal helices is derived from proline residues. Helix 1 is formed by six repeats of the Pro-X dipeptide, and the shorter helix 2 contains two such repeats. In both helices, only a few hydrogen bonds were found. Several changes in the N-extension were observed during molecular dynamics simulations (Figure 10). First, after structure equilibration for 20 ps, a partial "melting" of the proline-based helices occurred with a conformational change in a highly mobile loop region in which lysine 47 has a high solvent accessibility (Figure 10, inset). These structural features provide a basis for the susceptibility of this region to tryptic processing and for the in vivo processing by gelatinase B (*40*) and m-calpain (*41*). Furthermore, they indicate that the post-translational processing of the βB1 N-terminal extension is defined by its structure and conformation and not the specificity of any particular protease.

CONCLUSIONS

The crystallin N-terminal extensions are susceptible to temporal in vivo proteolytic processing, and this appears to impact protein interaction potentials. As the in vivo processing end points are variable (*40*, *49*−*51*), we used structural boundaries to define the lengths of the extensions. In βB1, removal of the extension strengthens the propensity for self-association, thus weakening or blocking its ability to participate in heteromolecular associations with βA3. Removal of the corresponding extension from βA3 has little effect on dimerization and did not block heteromolecular association with βB1. We have suggested that the N-terminal arms mainly influence initial homo- and heteromolecular dimerization and that interfaces in the main core domains mediate the higher-order associations. In vitro proteolytic processing of βB1 simulates in vivo processing and provided structure−function insight by showing that removal of more than 80% of the βB1 extension rather than inhibition of heteromolecular associations actually enhances them. Molecular modeling suggests that the βB1 N-terminus although largely disordered and flexible contains regions with helical propensity which position a flexible mobile loop region creating a protease "hot spot". Cleavage specificity is, thus, structure-driven, and the physiological significance of any one particular protease reported to process this region remains to be more clearly established. The structural significance of the small stretch of βB1 sequence of residues 48−56 also requires further investigation as its presence or absence has a profound effect on protein interactions.

ACKNOWLEDGMENT

We thank Dr. Oleg Voloshin (National Institute of Diabetes and Digestive and Kidney Diseases, National Institutes of Health) for assistance with circular dichroism and Dr. Fielding Hejtmancik (National Eye Institute, National Institutes of Health) for useful discussions and criticism. M.P.C. was supported by the Howard Hughes Medical Institute Research Scholars Program.

REFERENCES

1. Delaye, M., and Tardieu, A. (1983) Short-range order of crystallin proteins accounts for eye lens transparency. *Nature 302*, 415–417.
2. Wistow, G. J., and Piatigorsky, J. (1988) Lens crystallins: The evolution and expression of proteins for a highly specialized tissue. *Annu. Rev. Biochem. 57*, 479–504.
3. Bloemendal, H., de Jong, W., Jaenicke, R., Lubsen, N. H., Slingsby, C., and Tardieu, A. (2004) Ageing and vision: Structure, stability and function of lens crystallins. *Prog. Biophys. Mol. Biol. 86*, 407–485.
4. Lubsen, N. H., Aarts, H. J., and Schoenmakers, J. G. (1988) The evolution of lenticular proteins: The β- and γ-crystallin super gene family. *Prog. Biophys. Mol. Biol. 51*, 47–76.

5. Lampi, K. J., Oxford, J. T., Bachinger, H. P., Shearer, T. R., David, L. L., and Kapfer, D. M. (2001) Deamidation of human βB1 alters the elongated structure of the dimer. *Exp. Eye Res. 72*, 279–288.
6. Werten, P. J., Lindner, R. A., Carver, J. A., and de Jong, W. W. (1999) Formation of βA3/βB2-crystallin mixed complexes: Involvement of N- and C-terminal extensions. *Biochim. Biophys. Acta 1432*, 286–292.
7. Zigler, J. S. Jr., Horwitz, J., and Kinoshita, J. H. (1980) Human β-crystallin. I. Comparative studies on the β1, β2 and β3-crystallins. *Exp. Eye Res. 31*, 41–55.
8. Bindels, J. G., Koppers, A., and Hoenders, H. J. (1981) Structural aspects of bovine β-crystallins: Physical characterization including dissociation-association behavior. *Exp. Eye Res. 33*, 333–343.
9. Slingsby, C., and Bateman, O. A. (1990) Qarternary interactions in eye lens β-crystallins: Basic and acidic subunits of β-crystallins favor heterologous association. *Biochemistry 29*, 6592–6599.
10. Berbers, G. A. M., Boerman, O. C., Bloemendal, H., and de Jong, W. W. (1982) Primary gene products of bovine β-crystallin and reassociation behavior of its aggregates. *Eur. J. Biochem. 128*, 495–502.
11. Ajaz, M. S., Ma, Z., Smith, D. L., and Smith, J. B. (1997) Size of human lens β-crystallin aggregates are distinguished by N-terminal truncation of βB1. *J. Biol. Chem. 272*, 11250–11255.
12. Hanson, S. R., Hasan, A., Smith, D. L., and Smith, J. B. (2000) The major in vivo modifications of the human water-insoluble lens crystallins are disulfide bonds, deamidation, methionine oxidation and backbone cleavage. *Exp. Eye Res. 71*, 195–207.
13. Lampi, K. J., Ma, Z., Hanson, S. R., Azuma, M., Shih, M., Shearer, T. R., Smith, D. L., Smith, J. B., and David, L. L. (1998) Age-related changes in human lens crystallins identified by two-dimensional electrophoresis and mass spectrometry. *Exp. Eye Res. 67*, 31–43.
14. Han, J., and Schey, K. L. (2006) MALDI tissue imaging of ocular lens α-crystallin. *Invest. Ophthalmol. Visual Sci. 47*, 2990–2996.
15. Robinson, N. E., Lampi, K. J., Speir, J. P., Kruppa, G., Easterling, M., and Robinson, A. B. (2006) Quantitative measurement of young human eye lens crystallins by direct injection Fourier transform ion cyclotron resonance mass spectrometry. *Mol. Vision 12*, 704–711.
16. Sergeev, Y. V., David, L. L., Chen, H.-C., Hope, J. N., and Hejtmancik, J. F. (1998) Local microdomain structure of terminal extensions in βA3- and βB2-crystallins. *Mol. Vision 4*, 9.
17. Gupta, R., Srivastava, K., and Srivastava, O. P. (2006) Truncation of motifs III and IV in human lens βA3-crystallin destabilizes the structure. *Biochemistry 45*, 9964–9978.
18. Harding, J. J., and Crabbe, M. J. C. (1984) The lens. Development, proteins, metabolism and cataract. In The Eye (Davson, H., Ed.) 3rd ed., Vol. IB, pp 207−492, Academic Press, Orlando.
19. David, L. L., Lampi, K. J., Lund, A. L., and Smith, J. B. (1996) The sequence of human βB1-crystallin cDNA allows mass spectrometric detection of βB1 protein missing portions of its N-terminal extension. *J. Biol. Chem. 271*, 4273–4279.
20. Lampi, K. J., Ma, Z., Shih, M., Shearer, T. R., Smith, J. B., Smith, D. L., and David, L. L. (1997) Sequence analysis of βA3, βB3, and βA4 crystallins completes the identification of the major proteins in young human lens. *J. Biol. Chem. 272*, 2268–2275.
21. Takemoto, L., Takemoto, D., Brown, G., Takehana, M., Smith, J., and Horwitz, J. (1987) Cleavage from the N-terminal region of βBp crystallin during aging of the human lens. *Exp. Eye Res. 45*, 385–392.
22. Harrington, V., McCall, S., Huynh, S., Srivastava, K., and Srivastava, O. P. (2004) Crystallins in water soluble-high molecular weight protein fractions and water insoluble protein fractions in aging and cataractous human lenses. *Mol. Vision 10*, 476–489.
23. Berbers, G. A. M., Hoekman, W. A., Bloemendal, H., de Jong, W. W., Kleinschmidt, T., and Braunitzer, G. (1983) Proline- and alanine-rich N-terminal extension of the basic bovine β-crystallin B1 chains. *FEBS Lett. 161*, 225–229.
24. Werten, P. J. L., Carver, J. A., Jaenicke, R., and de Jong, W. W. (1996) The elusive role of the N-terminal extension of βA3- and βA1-crystallin. *Protein Eng. 9*, 1021–1028.
25. Sergeev, Y. V., Wingfield, P. T., and Hejtmancik, J. F. (2000) Monomer-dimer equilibrium of normal and modified βA3-crystallins: Experimental determination and molecular modeling. *Biochemistry 39*, 15799–15806.
26. Sergeev, Y. V., Hejtmancik, J. F., and Wingfield, P. T. (2004) Energetics of Domain-Domain Interactions and Entropy Driven Association of β-Crystallins. *Biochemistry 43*, 415–424.
27. Bateman, O. A., Lubsen, N. H., and Slingsby, C. (2001) Association behaviour of human βB1-crystallin and its truncated forms. *Exp. Eye Res. 73*, 321–331.
28. Annunziata, O., Pande, A., Pande, J., Ogun, O., Lubsen, N. H., and Benedek, G. B. (2005) Oligomerization and phase transitions in aqueous solutions of native and truncated human βB1-crystallin. *Biochemistry 44*, 1316–1328.
29. Kroone, R. C., Elliott, G. S., Ferszt, A., Slingsby, C., Lubsen, N. H., and Schoenmakers, J. G. (1994) The role of the sequence extensions in β-crystallin assembly. *Protein Eng. 7*, 1395–1399.
30. Liu, B. F., and Liang, J. J. (2007) Protein-protein interactions among human lens acidic and basic β-crystallins. *FEBS Lett. 581*, 3936–3942.
31. Jaenicke, R., and Slingsby, C. (2001) Lens crystallins and their microbial homologs: Structure, stability, and function. *Crit. Rev. Biochem. Mol. Biol. 36*, 435–499.
32. Hejtmancik, J. F., Wingfield, P., Chambers, C., Russell, P., Chen, H.-C., Sergeev, Y. V., and Hope, J. N. (1997) Association properties of βB2- and βA3-crystallin: Ability to form dimers. *Protein Eng. 10*, 1347–1352.
33. Takata, T., Woodbury, L. G., and Lampi, K. J. (2009) Deamidation alters interactions of β-crystallins in hetero-oligomers. *Mol. Vision 15*, 241–249.
34. Chan, M. P., Dolinska, M., Sergeev, Y. V., Wingfield, P. T., and Hejtmancik, J. F. (2008) Association properties of βB1- and βA3-crystallins: Ability to form heterotetramers. *Biochemistry 47*, 11062–11069.
35. Laue, T. M., Shah, B. D., Ridgeway, T. M., and Pelletier, S. L. (1992) Computer-aided interpretation of analytical sedimentation data for proteins. In Analytical Ultracentrifugation in Biochemistry and Polymer Science (Harding, S. E., Rowe, A. J., and Horton, J. C., Eds.) pp 90−125, Royal Society of Chemistry, Cambridge, U.K.
36. Ventura, S. (2005) Sequence determinants of protein aggregation: Tools to increase protein solubility. *Microb. Cell Fact. 4*, 11.
37. Scharnagl, C., Reif, M., and Friedrich, J. (2005) Stability of proteins: Temperature, pressure and the role of the solvent. *Biochim. Biophys. Acta 1749*, 187–213.
38. Lampi, K. J., Kim, Y. H., Bachinger, H. P., Boswell, B. A., Lindner, R. A., Carver, J. A., Shearer, T. R., David, L. L., and Kapfer, D. M. (2002) Decreased heat stability and increased chaperone requirement of modified human βB1-crystallins. *Mol. Vision 8*, 359–366.
39. Coop, A., Goode, D., Sumner, I., and Crabbe, M. J. (1998) Effects of controlled mutations on the N- and C-terminal extensions of chick lens βB1 crystallin. *Graefe's Arch. Clin. Exp. Ophthalmol. 236*, 146–150.
40. Descamps, F. J., Martens, E., Proost, P., Starckx, S., Van den Steen, P. E., Van, D. J., and Opdenakker, G. (2005) Gelatinase B/matrix metalloproteinase-9 provokes cataract by cleaving lens βB1 crystallin. *FASEB J. 19*, 29–35.
41. Shih, M., David, L. L., Lampi, K. J., Ma, H., Fukiage, C., Azuma, M., and Shearer, T. R. (2001) Proteolysis by m-calpain enhances in vitro light scattering by crystallins from human and bovine lenses. *Curr. Eye Res. 22*, 458–469.
42. Hope, J. N., Chen, H. C., and Hejtmancik, J. F. (1994) βA3/A1-Crystallin association: Role of the amino terminal arm. *Protein Eng. 7*, 445–451.
43. Bateman, O. A., Sarra, R., Van Genesen, S. T., Kappe, G., Lubsen, N. H., and Slingsby, C. (2003) The stability of human acidic β-crystallin oligomers and hetero-oligomers. *Exp. Eye Res. 77*, 409–422.
44. van Montfort, R. L., Bateman, O. A., Lubsen, N. H., and Slingsby, C. (2003) Crystal structure of truncated human βB1-crystallin. *Protein Sci. 12*, 2606–2612.
45. Norledge, B. V., Trinkl, S., Jaenicke, R., and Slingsby, C. (1997) The X-ray structure of a mutant eye lens βB2-crystallin with truncated sequence extensions. *Protein Sci. 6*, 1612–1620.
46. Trinkl, S., Glockshuber, R., and Jaenicke, R. (1994) Dimerization of βB2-crystallin: The role of the linker peptide and the N- and C-terminal extensions. *Protein Sci. 3*, 1392–1400.
47. Bergdoll, M., Remy, M. H., Cagnon, C., Masson, J. M., and Dumas, P. (1997) Proline-dependent oligomerization with arm exchange. *Structure 5*, 391–401.
48. Nalini, V., Bax, B., Driessen, H., Moss, D. S., Lindley, P. F., and Slingsby, C. (1994) Close packing of an oligomeric eye lens β-crystallin induces loss of symmetry and ordering of sequence extensions. *J. Mol. Biol. 236*, 1250–1258.
49. David, L. L., Shearer, T. R., and Shih, M. (1993) Sequence analysis of lens β-crystallins suggests involvement of calpain in cataract formation. *J. Biol. Chem. 268*, 1937–1940.
50. David, L. L., and Shearer, T. R. (1993) β-Crystallins insolubilized by calpain II in vitro contain cleavage sites similar to β-crystallins insolubilized during cataract. *FEBS Lett. 324*, 265–270.

51. Shih, M., Lampi, K. J., Shearer, T. R., and David, L. L. (1998) Cleavage of β-crystallins dring maturation of bovine lens. *Mol. Vision 4*, 4.
52. Srivastava, K., Gupta, R., Chaves, J. M., and Srivastava, O. P. (2009) Truncated Human B1-Crystallin Shows Altered Structural Properties and Interaction with Human A3-Crystallin. *Biochemistry 48*, 7179–7189.
53. Evans, P., Bateman, O. A., Slingsby, C., and Wallace, B. A. (2007) A reference dataset for circular dichroism spectroscopy tailored for the $\beta\gamma$-crystallin lens proteins. *Exp. Eye Res. 84*, 1001–1008.
54. Srivastava, O. P., Kirk, M. C., and Srivastava, K. (2004) Characterization of covalent multimers of crystallins in aging human lenses. *J. Biol. Chem. 279*, 10901–10909.
55. Ma, Z., Hanson, S. R., Lampi, K. J., David, L. L., Smith, D. L., and Smith, J. B. (1998) Age-related changes in human lens crystallins identified by HPLC and mass spectrometry. *Exp. Eye Res. 67*, 21–30.
56. Griko, Y., Sreerama, N., Osumi-Davis, P., Woody, R. W., and Woody, A. Y. (2001) Thermal and urea-induced unfolding in T7 RNA polymerase: Calorimetry, circular dichroism and fluorescence study. *Protein Sci. 10*, 845–853.